

IN SITU FOURIER-TRANSFORM INFRARED SPECTROSCOPY STUDIES OF INORGANIC IONS ADSORPTION ON METAL OXIDES AND HYDROXIDES

G. Lefèvre

Centre d'Etudes de Chimie Métallurgique CNRS-UPR 2801
15, Rue Georges Urbain F94407 Vitry/Seine
France

lefevre@glvt-cnrs.fr
Fax: 33-1-46-75-04-33

ABSTRACT

In this work, the studies describing the use of attenuated total reflection – infrared spectroscopy to obtain information on the sorption mechanism of inorganic ions on metal oxy-hydroxides are reviewed. ATR-IR is amongst the rare techniques which allow to analyze the sorption phenomena *in situ* and led to several results about the speciation of sorbed anions (sulfate, carbonate, phosphate, perchlorate, ...) or ternary inorganic complexes since it is able to distinguish outer-sphere and inner-sphere complexes. The principles of this method are summarized, and the experimental protocols, the results and the limitations are detailed. The sample deposition method, initially based a paste or a concentrated suspension, have evolved towards the coating of the ATR crystal by a colloid layer, increasing the sensibility and the reproducibility of the measurements. Observed absorption frequencies of ions sorbed on metal oxy-hydroxides (goethite, hematite, alumina, silica, TiO₂, ...) are reported to help the identification of peaks in new experimental works. This method, characterized by an *in situ* analysis performed with a special cell used in a widespread instrumentation (IR spectrometer), is very recent but its advantages suitable for the current problems in the sorption field should help its rapid development for the next years.

ATR-IR; surface complexation; review; oxides, hydroxides; sorption

INTRODUCTION

Sorption of inorganic ions on solid matter plays a major role in several fields such as catalysis, transport of toxic species in natural waters, and decontamination of liquid wastes. The long-term safety of radioactive waste depositories is based on the sorption of radionuclides on engineered and natural barriers placed around the depositories. In order to predict the safety of such depositories in very long term, it is necessary to extrapolate sorption data, measured on reference systems at the laboratory scale, to real systems and over very long times. Thus the extrapolation of data measured in laboratory studies must be performed through models based on physico-chemical processes as close as possible to the real ones. If a process that may become important at a certain moment is ill modeling or forgetting, the long-term prediction may turn out to be wrong. Thus, the determination and modeling of the sorption mechanisms, connected to the long-term safety of radioactive waste depositories, has become a great challenge.

Several methods of modeling sorption data have been developed. The simplest one is the measurement of the distribution coefficient (K_D) of ions between the solution and a mineral, and the further use of K_D data banks to calculate the retardation factors of radionuclides during the water transport. However, since K_D values depend on many factors, this method is very hazardous. Modeling of adsorption isotherms by Langmuir equations allows calculating an affinity constant (K_{ads}) [1]. At low concentrations, K_{ads} is related with K_D by the formula $K_D = K_{ads} \times c_{max}$ where c_{max} is the maximum surface concentration (mol/kg). Other models are used to fit experimental adsorption isotherms, in order to take into account lateral interactions (Frumkin equation) or heterogeneous surface properties (Freundlich equation) [1]. The surface complexation models, based on chemical and electrostatic processes at the solid-water interface, would be a better way to quantify the sorption processes. However, the choice between several surface complexation models (1-pK or 2-pK monosite models, 1-pK multisite

model), together with the choice of the right electrostatic model [2,3], are still a matter of a large debate. These problems will not be detailed in this review, which deals with another important information: the nature of species sorbed at the water-solid interface. The surface speciation is of the utmost importance when determining thermodynamic surface complexation constants. Differentiating between inner- (IS) and outer-sphere (OS) complexes has been often made by observing the effect of ionic strength on the quantity of sorbed ions. However, this method has been questioned in several papers [4,5], pointing out the need of spectroscopic methods to solve this problem. The fitting of experimental data, as the sorbed fraction of ions versus pH, has been used to determine both the surface inner-sphere complex structure (typically monodentate or bidentate) and the thermodynamic complexation constant [3]. However, due to the number of adjustable parameters (sites density, acidity constants, surface complexation constants, electrostatic parameters,...), such a method often led to several sets of surface complexes [3] and spectroscopic results may be of invaluable help for determining the nature of surface complexes.

Ex-situ spectroscopic methods have been used to characterize the surfaces of metallic oxy-hydroxides after sorption. X-ray photoelectron spectroscopy (XPS) brings information on the oxidation state of the sorbed ions (which can be different from the solute species if a redox reaction occurs [6]), and may distinguish different surface complexes through the shift of the binding energy for ions such as uranyl [7], but this method is not efficient for most of the elements due to the small variations in the chemical environment of elements induced by the surface complexation. Moreover, this method is performed inside a high vacuum chamber, and dehydration may modify the structure of surface complexes.

X-ray absorption spectroscopy (XANES, EXAFS) is the most widespread technique used to investigate the surface complexes geometry on wet samples. The determination of coordination numbers of the sorbed ion and radial distances of the shells surrounding it have

led to interesting results, for instance on goethite reactivity towards Se [5] or Pb [8], or on the reactivity of alumina surface towards As [9], Cd [10] or Se [10].

Due to its ability to probe chemical bonds, infrared spectroscopy has been applied for years to sorption studies. The first studies made use of invasive sampling techniques, in which dried compacted powders (transmission spectra) or mixtures with KBr (diffuse reflectance spectra: DRIFT) were analyzed. Drying samples has been suggested to favoring the conversion of monodentate to bidentate complexes of sulfate [11,12], whereas Sugimoto and Wang [13] attributed this behavior to a pH drop during the drying process. Moreover, dilution in KBr in presence of trace of wetness would result in pH shifting towards neutral values [11], converting IS sulfate sorbed at low pH values to OS complex. Since ions might be coordinated differently with dried and wet surfaces, FTIR measurements in the presence of water are needed. The problem of the strong IR absorption by water could be believed as irresolvable. This problem can be solved by using internal reflection spectroscopy, i.e. by probing a short depth of sample by the evanescent wave existing in a lower index refraction medium (water) in contact with a more dense medium in which an IR radiation is propagating [14]. This spectroscopic technique, called attenuated total reflection (ATR), was firstly applied to the sorption of organic molecules onto suspensions in relation with flotation process [15], but several factors, as the impact of surface charge on dispersitivity, complicates quantitative measurements in suspensions with changing parameters (pH, adsorbate concentration, ionic strength). Its use to characterize the surface complexes of inorganic ions sorbed onto oxides has gained advantage from the procedure developed by Hug and Sulzberger [12,16] who coated the ATR element by a layer of colloidal mineral particles, allowing a quantitative spectral analysis.

This review will address the current state of knowledge in the use of FTIR-ATR to determine surface complexes between inorganic ions and oxides/hydroxides surfaces. Several

more general reviews about ATR have previously been published [15,17,18], but the objective of this work is to gather the experimental protocols used by the few groups currently working in this field, the results they obtained, and the limitations of this method.

ATTENUATED TOTAL REFLECTION SPECTROSCOPY

Principles

Internal reflection spectroscopy is based on the existence of an evanescent wave in a medium of lower index of refraction in contact with an optically denser medium in which a light is introduced [14]. This evanescent field decays exponentially in the rarer medium according to equation (1), so that the light probes only the first micrometers of this medium [16,19]:

$$E = E_0 \exp\left[-\frac{2\pi}{\lambda_1} (\sin^2 \theta - n_{21}^2)^{1/2} Z\right] = E_0 \exp(-\gamma Z) \quad (1)$$

where $\lambda_1 = \lambda / n_1$ is the wavelength of the radiation in the denser medium, λ is the wavelength in free space, θ is the angle of incidence with respect to the normal, $n_{21} = n_2 / n_1$, where n_1 and n_2 are respectively, the refractive index of the optically denser and rarer medium, and Z is the distance from the surface [14] (see Fig. 1).

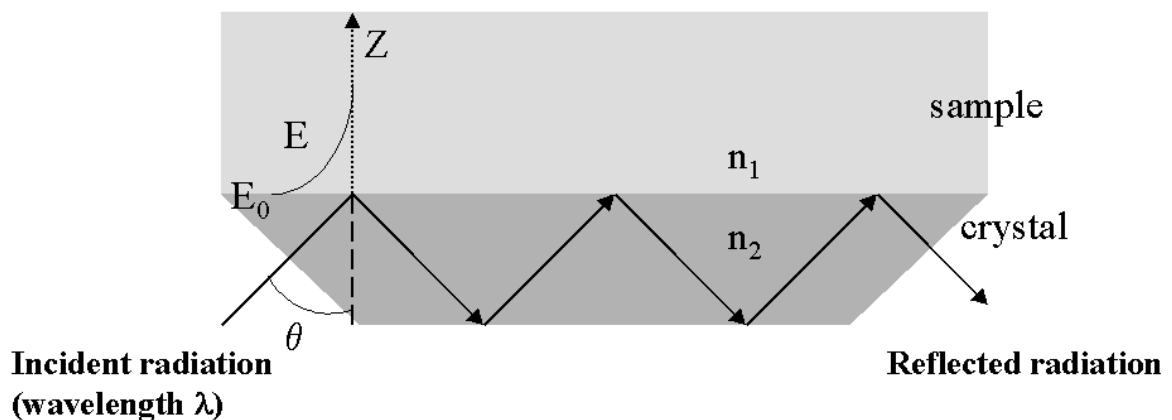


Fig. 1. Schematic diagram of a horizontal sampling accessory illustrating the parameters of significance to evanescent wave. Adapted from Hind et al. [17].

If the sample absorbs radiation, the reflected wave becomes attenuated, and its reflectance is expressed as follows for N reflections:

$$R^N = (1 - \alpha d_e)^N \quad (2)$$

where d_e is the effective path length and α the absorptivity of the layer. d_e is defined as the thickness required to obtain the same absorption in transmission measurement as that obtained in reflectance experiment.

From equation (1), different parameters can be defined to characterize the depth of penetration. The earlier definition was the depth at which electric field amplitude falls to half its value at the surface ($Z = 0.69 / \gamma$), but the current definition of the depth of penetration (d_p) is the value of $Z = 1 / \gamma$, therefore a decay of the electric field of 63 %. Moreover, this value is lower than the actual depth sampled (d_s), which was about three times d_p (decay of the electric field of 95%) [14,20]. Equation (1) can be used to obtain the value of d_p in a homogeneous solution, but there is a great concern for the determination of depth of penetration through oxy-hydroxide films.

Indeed, when studying the ions adsorbed on layers of particles deposited on ATR crystals, it is interesting to know if the whole layer is probed. Hug and Sulzberger [16] have applied the formula (1) with a volume-weighted average of the refractive index of the particle material and the aqueous solution:

$$n_2 = F_v \times n_{\text{par}} + (1 - F_v) \times n_{\text{water}} \quad (3)$$

where F_v is the volume fraction of solid and n_{par} the refractive index of the pure solid. This water content is required to explain the possibility of using ATR spectroscopy on layers of solids whose refractive indexes (RI) are greater than those of ZnSe (2.4), as hematite (RI ~

3 [21]) or anatase (RI of 2.6 [22]). The depth of penetration, d_p , is expressed as (from the review by Coates [19]):

$$d_p = \frac{\lambda_1}{2\pi} (\sin^2 \theta - n_{21}^2)^{-1/2} \quad (4)$$

or, with ν , the frequency in wavenumbers (cm^{-1}):

$$d_p = \frac{10000}{2\pi\nu n_1} (\sin^2 \theta - n_{21}^2)^{-1/2} \quad (5)$$

From the mass of TiO_2 deposited on the crystal and its thickness ($1.7 \pm 0.3 \mu\text{m}$) measured with an atomic force microscope, a volume fraction between 0.30 and 0.40 was calculated, leading to d_p values between 2 and 2.6 μm (Table 1). The actual depth sampled would be *ca.* 6 μm ($d_s = 3 \times d_p$), larger than the layer thickness. It is noteworthy that the refractive index of the particles layer is larger than those of bulk water ($n_{\text{water}} = 1.34$), leading to a deeper penetration in the particle layer. In a work on hematite properties, Hug [12] compares the penetration depth in H_2O (1.39 μm at 1100 cm^{-1}) with the thickness of the particle layer and conclude that the entire Fe_2O_3 layer is probed. From the values of θ and Fe_2O_3 density given in this article [12] and the refractive index of hematite ($n_2 \sim 3$ [21]), the condition of internal reflectance, expressed as $(\sin^2 \theta - n_{21}^2) \geq 0$, leads to an upper limit value for n_2 of $2^{-1/2} \times n_{\text{ZnSe}} = 1.70$, corresponding to a maximum volume fraction of solid (F_v) of 0.22, despite that the given density of loose particle layer (2 g.cm^{-3}) leads to a slightly larger value (0.24). The calculation of the penetration depth in the particles layer d_p for an angle of incidence close to the limit gives large values, and the penetration of the evanescent wave is always less deep in bulk water than in a loose particles layer, for the usual case of a refractive index of the bulk solid higher than that of water. The value of $3 \times d_p$ for bulk water, *ca.* 4 μm at 1100 cm^{-1} , may be considered as the upper value for the thickness of a deposited film, to ensure the sampling of the whole layer. This value is lower than the usual thickness of layers, and the calculation of the d_p in the particles layer would be needed only if a thicker layer is

deposited, all the more so that the presence of particles increases the penetration depth (table 1).

Table 1. Penetration depth at 1100 cm^{-1} (d_p) in a layer of TiO_2 , and parameters used in its calculation: volume fraction of solid (F_v), layer thickness (d) and refractive index of the layer (n_2) (from Hug and Sulzberger [16], the refractive index was erroneously named n_1 in the original table).

d (μm)	F_v	n_2	d_p (μm)
2.00	0.30	1.53	2.01
1.72	0.35	1.57	2.25
1.50	0.40	1.60	2.61

Crystals

There is a wide choice of crystals for ATR spectroscopy, explained by the diversity of the fields where this technique is used (biology, semiconductor technology, earth sciences,...). For the application of in situ investigation of solid/solution interfaces, two main characteristics are required to choose a material: its resistance to solutions with mild acid-base characteristics (pH 4-10) and a low transmission threshold since the lowest vibrations of sorbed ions (Se-O, As-O) takes place around 750 cm^{-1} . In most of the published studies [4,11,12,23-32], ZnSe was used, the other materials were AMTIR (Amorphous Material which Transmits Infrared Radiation) [33,34], Ge [12,27] and diamond [35]. A summary of the properties of these materials can be seen in Table 2. Other materials (KRS-5, Si,...) have major drawbacks such as solubility in water or small transmission range.

Table 2. Properties of materials used for ATR crystals [17,19]

Material	Refractive Index	Chemical resistance	Mechanical resistance	Transmission threshold (cm ⁻¹)
ZnSe	2.4	etched by diluted acids and bases, eroded by zinc complexants	easily cracked	650
AMTIR	2.5	attacked by bases and oxidizing acids	very brittle	750
Ge	4.0	resistant to diluted acids and bases	brittle	870
Diamond	2.4	suitable to pH 1 to 14	very hard	< 200

Cells and methods of solid deposition

Two methods were used to bring particulate matter into contact with the crystal: (1) spreading a concentrated suspension [4,25,31] or a paste [27,29,33,34,36] on the crystal or (2) coating by colloidal particles to form a film stable toward stirring or flowing of the solution in direct contact. [11,12,16,23-26,28,32]. For the first method, the equilibrium of the system solid/solution is reached by a classical batch experiment, then the suspensions are centrifugated to obtain a suspension with a high mass/volume ratio. Samples as suspensions of 100-1000 g/L of oxides, or as a paste covering the entire crystal spread by means of a plastic spatula [33], are analyzed. Hug and Sulzberger [16] have pointed out several factors which complicate quantitative measurements by this method, as the dependence of the concentration of particles in the proximity of the ATR element on pH and surface coverage with adsorbate. This point was detailed by Tickanen et al. [20] who propose a methodology for determining the concentration of suspended goethite particles sampled by the evanescent wave from a cylindrical internal reflection (CIR) element. On the other hand, the paste method allow easily to determine the surface coverage, and the spectroscopic results can straightforwardly used in surface complexation modeling. The drawback of the layer method is a possible effect of the

structure of the colloid deposit on the surface reactivity and accessibility, hindering the comparison with results obtained on the well-dispersed colloidal suspension.

In order to increase the surface probed by the evanescent light and to avoid the problem of changing dispersivity of particles in suspension, Hug and Sulzberger [12,16] have performed the coating of the crystal with a stable layer of colloidal oxy-hydroxides particles. This method, modified by Peak et al. [11], begins by the synthesis of solids with high specific surface areas in suspension. Then, Hug [12] has prepared hematite layers as follows: “20 μ L Fe₂O₃ suspension (containing ca. 3.2 mg Fe₂O₃) mixed with 20 μ L ethanol was distributed over the ATR crystal. After drying, the layers were rinsed with H₂O until no more Fe₂O₃ detached”. For goethite film, Peak et al. [11] have described their method: “500 μ L of 0.01M NaCl adjusted to pH 4.5 was pipetted onto the crystal, forming a large droplet. Then, 10 μ L of a 250 g.L⁻¹ goethite suspension was placed into the center of the droplet with a pipette. The suspension was then mixed and spread evenly across the surface of the crystal using the pipette tip and allow to dry. Once the deposit was dry, it was rinsed by holding it at an angle, placing a large drop of 0.01 M NaCl onto one edge, and allowing the droplet to slowly move across the deposit. At the end, the excess electrolyte was absorbed with a KimWipe”. Hug [12] has estimated that 10-20% of initially deposited solid remained after rinsing, but Peak et al. [11] have weighed the crystal after deposition and found that all the goethite added forms a deposit. The difference between rinsing techniques may explain these opposite values.

No study on the characteristics of the film deposit on the ATR crystal was published, but films of colloids deposited in the same manner into other smooth supports were characterized by Degenhardt and McQuillan [24] who have studied a film of chromium hydroxide sol evaporated onto glass by SEM. It consists of a patchy multilayer of particles whose average diameter was 430 nm, and was about 2.5 μ m thick. Connor et al. [37] have observed by SEM layers of ZrO₂, TiO₂ and Al₂O₃ evaporated onto an aluminum disc. The film consists in flakes

of solid, whose thickness is less than 1 μm , separated by vacuum-formed cracks. Thus, before placing under vacuum, this film should continuously coated the support. Thickness of the films was characterized or calculated for several solids as hematite (0.2-0.4 μm [12]), TiO_2 ($1.7 \pm 0.3 \mu\text{m}$ [16] or 1 μm [26,37]), ZrO_2 (1 μm [37]), Al_2O_3 (1 μm [37]), Cr(III) oxy-hydroxide (2.5 μm [24]) or silica (1 μm [26]). In all cited cases, the entire layer should be probed by the evanescent wave (see *principles* part).

Other methods have been developed to obtain an oxide layer on an ATR substrate in relation with optical sensors of molecules in aqueous media [38,39]. Thus, sol-gel precursors of SiO_2 was found suitable producing thin (1.7 μm) homogeneous films on ZnSe [38]. Ninness at al. [39] have presented a technique using a binder (polyethylene) to anchor colloidal silica particles on ZnSe. The coating layer (about 5 μm in thickness) consisted in islands of 20 μm in size, separated by 5 μm cracks. Gas-phase reactions with silanes were used to evaluate the accessibility of the surface of silica, indicating that most of the hydroxyl groups are reactive.

Once the modified ATR crystal was prepared, it was generally placed into a flow cell (excepted in studies by Wijnja and Shulthess [25] and Gong [26] where static cells were used). The diagram of the experimental apparatus designed to study the interactions between the film of metal oxy-hydroxide and solution species (including protons) is shown in Fig. 2. The composition of the solution which flows onto the ATR crystal are changed by adding concentrated solutions of acid, base or adsorbing species in the reservoir (500 mL vessel), where the pH is measured. The flow rate value varied from 1 $\text{mL}\cdot\text{min}^{-1}$ to 7 $\text{mL}\cdot\text{min}^{-1}$ [16,23,24,28,30,32].

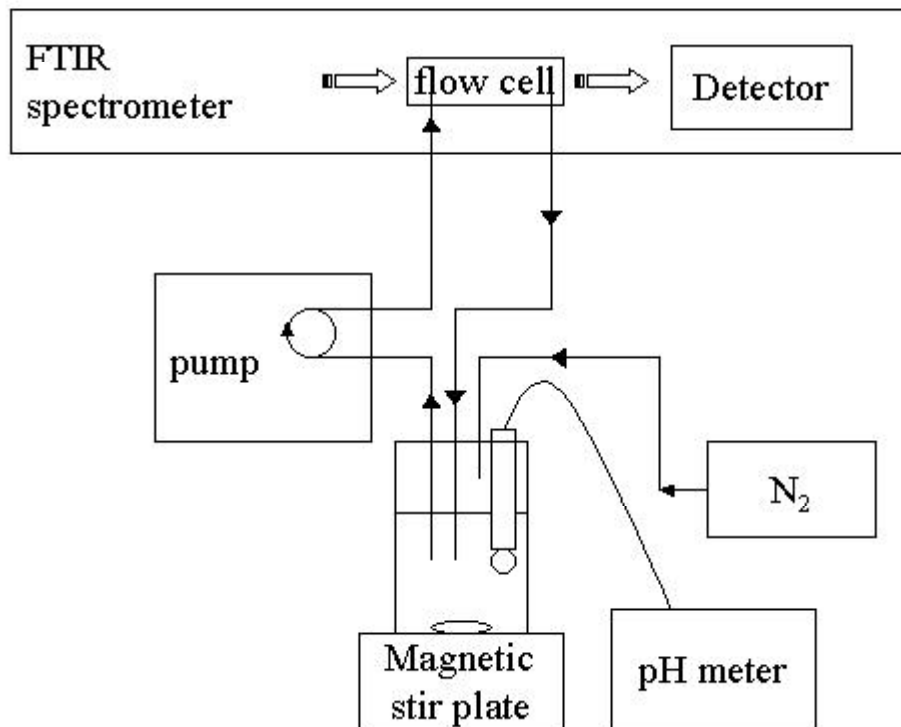


Fig. 2. Experimental apparatus used for pH envelopes and adsorption isotherms.

Adapted from Peak et al. [11]

A cell with a horizontal trough configuration was generally used, equipped with a crystal with coated upper face. Considering the adhesion strength of solid particles, a crystal with both sides coated may be used surrounded by solution, however, the author is unaware of any reported interfacial investigation using such a cell. Its advantage would be an increased sensitivity (almost twice) compared to single-coated crystals despite of some experimental complications.

Solution

The ionic strength of solutions is usually kept constant in sorption experiments, since it has an impact on the activity coefficients of aqueous species, but yet more on the surface charge of the solid particles. Ions considered to be inert, or non-sorbing on solid surfaces, are used as background electrolyte: Na^+ , K^+ , Cl^- , NO_3^- and ClO_4^- [40]. Due to the absence of absorption in mid-IR range, Cl^- was used in most of the ATR experiments [4,11,16,23,25, 27,29-31,33]. In spite of the bands of NO_3^- ($\sim 1300 \text{ cm}^{-1}$) and ClO_4^- ($\sim 1100 \text{ cm}^{-1}$), sodium salts of these ions were used in studies involving metal ions (respectively U(VI) [36] and Pb(II) [34]) to avoid the formation of chloride complexes. However, the inert electrolyte must be carefully chosen in function of the solid since specific adsorption of Cl^- was mentioned on γ -alumina [41] and Cu_2O [42]. The *iep* (isoelectric point determined by electrophoretic measurements) and *pzse* (point of zero salt effect: common intersection point of the acid-base titrations curves at different ionic strengths) of goethite [43], haematite [44] or anatase [45] did not vary systematically as a function of the chloride concentration what is an element in favor of a non-specific adsorption, although Rietra et al. [43] have shown that chloride was more able to screen the positive charge of goethite than nitrate or perchlorate, leading to a higher amount of sorbed protons and decreasing the sulfate uptake. A stronger effect of chloride on proton adsorption has been found for RuO_2 [46]. Bromide and iodide species seems to have less affinity for surface sites than chloride, on alumina [41,47] and anatase [45]. KBr was used [26,48] in the study of phosphate sorption on titania by ATR. In spite of the decrease of their reactivity, bromide and iodide have been scarcely used in sorption experiments as background electrolyte, and most of the published studies were carried out with Cl^- , NO_3^- and ClO_4^- . The comparison of ATR results with previous studies is therefore easier for Cl^- background electrolyte when studying the surface reactivity of iron oxyhydroxides.

Concentration of the dissolved species in equilibrium with the sorbed fraction on solid particles is another characteristic of the solution. The numerous applications of solid/solution researches in the field of environment pollution deal with concentrations spanning several orders of magnitude, from traces of radioactive ions to values greater than 0.01 M near dissolving fertilizer particles [49] (phosphate), or in acid mines drainage water [50] (sulfate). A hint for relevant concentrations range for environmental studies may be found in the limit concentration of pollutants as defined by the European directive on the quality of water [51]. For example, maximum concentrations in water intended for human consumption are 10 ppb for As and Se ($\sim 0.13 \mu\text{M}$), and 50 ppm for NO_3^- (0.81 mM) [51]. The sensitivity of ATR-IR, as other surface analysis methods, depends on the surface coverage with adsorbate. The experimental apparatus (Fig. 2) used for adsorption isotherms on particles layer leads to a high volume/mass ratio, thus a high coverage can be obtained with low dissolved concentrations. Moreover, ATR-IR sensitivity to sorbed oxoions is very dependent on the contact between the particulate matter and the crystal. Thus, crystals coated according to Hug's method [12,16] have allowed studies with sulfate or arsenate concentrations lower than $10 \mu\text{M}$ [11,12,16,28], whereas analysis of slurry have been performed with adsorbate concentrations between 1 mM and 0.5 M [4,29]. The sorption process allows to increase the signal of the ions by a huge factor, in comparison with dissolved species, and this characteristic has been used to develop sensors [38] to monitor organophosphates in natural waters down to sub-ppm concentration range.

Other parameters play a role in the sensitivity of the analysis, as the number of internal reflections, the specific area of the solid or the absorptivity of the detected ion. The pH values in the published works were in the range 3 – 9 (until 2-11 in a few works [22,24]), correlated to the ZnSe chemical resistance. This range corresponds to the usual pH values of sorption

studies, although the ZnSe resistance may limit the study of the surface reactivity at pH values higher than the *iep* of iron and aluminum oxy-hydroxides ($\sim 8 - 10$).

Solids

The majority of studies have involved high surface area solids, to increase the likelihood of obtaining good contact and to allow the probing of a high amount of sorbed species [17]. It is the case of goethite, whose specific surface area varies between 50 and 100 m²/g as a function of the parameters of its synthesis, which has been the subject of a number of studies [4,11,20,23,25,30,31,33,34,52,53]. Colloidal hematite (particle size 10-25 nm) and titania (particle size 20-30 nm), whose geometrical specific surface areas are higher than 50 m²/g, are the first solids that have been used to coat ATR crystals [12,16]. Amorphous metallic oxy-hydroxides are known to have even higher specific surface areas, as the compounds of iron (ca. 250 m²/g [4,27,29,31]) or aluminum (130 m²/g [29,31]).

RESULTS

Due to the principle of IR spectroscopy, only polyatomic ions can be probed by this method, by the M-O vibrations (where M represents S, C,...). Thus, studies can be carried out on a limited number of inorganic oxoanions whose free ion is detected between 1500 cm⁻¹ (carbonate) and ca. 750 cm⁻¹ (selenite) (see Table 3). The transmission threshold of the crystal material determines the lowest wavenumbers which can be measured, so the use of materials with high thresholds (Ge for example) prevents from studying “heavy” oxoanions, since the stretching vibrations reach low wavenumbers for heavy element (as illustrated by the

comparison between SO_4^{2-} and SeO_4^{2-} in Table 3). The strong absorption of H_2O below 800-850 cm^{-1} limit studies with this solvent, but this limit can be decrease by ca. 100 cm^{-1} in D_2O .

Table 3. Positions of peak maxima of dissolved and coordinated anions

species* (reference)	Infrared active band positions (cm^{-1}) **							
	800		1000		1200		1400	
SO_4^{2-} [12,24,25]					1100			
HSO_4^- [12]		890		1050		1195		
hematite-sulfate [12]			975		1060	1130		
goethite-sulfate [11]			975		1055	1135		
goethite-sulfate [25]			975		1055	1130		
COH-sulfate [24]			980		1060	1120		
ClO_4^- [24]						1105		
COH-perchlorate [24]						1105		
TiO_2 -perchlorate [22]						1104		
$\text{S}_2\text{O}_3^{2-}$ [24]			995			1115		
COH-thiosulfate [24]			995			1105		
AsO_4^{3-} [28]	790							
HAsO_4^{2-} [28]		860						
H_2AsO_4^- [28]	740	880	910					
HFO-arsenate [28]	825							
$\text{B}(\text{OH})_4^-$ [29]				955		1170		
$\text{B}(\text{OH})_3^0$ [29]						1150		1410
HAO-borate [29]	-	-	-	-	-		1280	1420
HFO-borate [29]				985		1255	1295	1400
PO_4^{3-} [27,52]					1005			
HPO_4^{2-} [27,52]	850	890		990		1075		
H_2PO_4^- [27,52]	875		940			1075	1155	
H_3PO_4 [27,52]		890			1005		1175	1250
goethite-phosphate [52]	-	-	-	-	1005	1045	1100	1120
TiO_2 -phosphate [32]				985	1030		1100	
TiO_2 -phosphate [26]			915	980	1010	1055	1115	
FH-phosphate [27]			950		1020	1090		
CO_3^{2-} [31]		885				1065		1385
HCO_3^- [31]	845				1010		1310	1360
HAO-carbonate [31]	-	-	-	-	-	1030		1420
γ alumina-carbonate [54]	-	-	-	-				1490
γ alumina-carbonate [54]	-	-	-	-			1390	1510
HFO-carbonate [31]						1070	1335	1410
hematite-carbonate [36]							1350	1500
goethite-carbonate [33]	-	-	-	-			1335	1490
SeO_4^{2-} [4]			870					
SeO_3^{2-} [4]	730	825	850					
goethite-selenate [55]		820	850	880				
HFO-selenate [4]				885	895			
HFO-selenite [4]	750	845						
NO_3^- [54]							1350	
γ alumina-nitrate [54]	-	-	-	-			1350	

* abbreviations of the names of solid phases: COH = Cr(III) oxide hydroxide, HFO = amorphous ferric oxide, HAO = amorphous aluminum oxide, FH = ferrihydrite; ** range where absorption bands of the solid phases prevent the detection of sorbed species is dotted

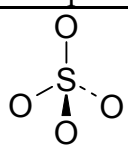
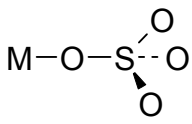
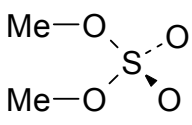
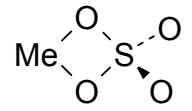
Moreover, the symmetry of these ions is lowered when they sorbed onto minerals surface via an inner-sphere complex, leading to a peak split of ca. 150 cm^{-1} for carbonate [33] and sulfate [12] for example. This effect must be taken into account when planning to study oxoanions whose vibration of free species is close to the transmission threshold of the ATR crystal or of the solvent. On the other hand, the outer-sphere sorption, as illustrated by perchlorate ion, has a weak impact on the ion symmetry and no change may be expected between vibration wavenumbers of free and sorbed ion.

Sulfate

The adsorption mechanism of sulfate ions onto oxides was not been resolved during years. The main issue was to determine if sulfate is sorbed as an inner-sphere (IS) or an outer-sphere (OS) complex. From macroscopic experiments, it was observed that ionic strength has a large effect on the fraction of sulfate that is adsorbed onto goethite [56], what have led Perrson and Lövgren [56] to model this sorption by two OS complexes ($\equiv\text{FeOH}_2^+\text{SO}_4^{2-}$ and $\equiv\text{FeOH}_2^+\text{HSO}_4^-$). However, sulfate adsorption shifts the point of zero charge of goethite to higher values, which is characteristic of an IS complex. The use of *in situ* ATR-FTIR spectroscopy have brought new elements to understand this problem. The infrared spectra of sulfate species relates to the symmetry of the complex, as shown in table 4. Sulfate in solution belongs to the point group T_d , and only one peak at ca. 1100 cm^{-1} is observed, corresponding

to the triply degenerate asymmetric stretching vibration (ν_3). Complexation of the sulfate ion lowers its symmetry, leading to a split of the ν_3 in two (for C_{3v} point group) or three (C_{2v} or C_1) peaks while the symmetric stretching ν_1 becomes active around 950 cm^{-1} . As shown by the bands of sulfate/cobalt complexes, the characterization of the ν_3 split may determine the structure of the surface complex, i.e. monodentate or bidentate.

Table 4. Positions of peak maxima of dissolved sulfate and Co(III) sulfato complexes

Species geometry	Symmetry	IR active bands				Species
 aqueous sulfate	T_d	1100				SO_4^{2-} [12]
 Monodentate (M = metal or proton)	C_{3v}	891	1051	1194	HSO_4^- [12]	
		970	1038	1130	$[Co(NH_3)_5SO_4]Br$ [57]	
		978	1070	1130	$[Co(en)_2(H_2O)SO_4]Br$ [58]	
 Bidentate binuclear	C_{2v}	995	1055	1105	$[(NH_3)_4Co]_2\mu(SO_4, NH_2)$ [57]	
		1170				
 Bidentate mononuclear	C_{2v}	995	1075	1176	$[Co(en)_2SO_4]Br$ [58]	
		1211				

Infrared spectroscopies have led to opposite results too, since a bidentate binuclear complex was identified by FTIR [59], whereas an OS complex was shown by DRIFT [56]. It is noteworthy that the analyzed samples were potentially altered by drying or dilution in a salt that may modify the structure of the original surface complex. The conclusion of ATR-IR experiments is that sulfate adsorption on goethite [11] occurs via both OS and IS complexation. On amorphous chromium (III) oxy-hydroxide [24], the signal of sorbed sulfate was interpreted as an OS complex due to the lack of a clear split of the absorption band.

However, the asymmetry of the peak for the lowest pH may suggest the contribution of an IS complex, which would have a weak contribution to the total signal. On hematite [12], the sorption takes place mainly by IS complexation, with a contribution of an OS complex for pH 5 – 7. Experiments on the adsorption of sulfate have been also carried out on TiO₂ (anatase) [16]. Despite the large contribution of the sulfate species present in the solution, what complicates the spectra, the absorption signal reveals two shoulders on either side of the main peak, ascribed to the split due to an IS complex. In conclusion, the results obtained by this method has pointed out the possibility for an ion to sorb via both OS and IS complexation reaction. This possibility, even if it is not surprising, have been rarely suggested due to the lack of other experimental methods to highlight this behavior. ATR-FTIR spectroscopy allows the simultaneous detection of the both kinds of complexes, but the decomposition of the signal remains tricky. Thus, Hug and Sulzberger [16] have found that the signal of sulfate adsorbed onto TiO₂ may be reconstructed from three peaks corresponding to the contribution of sulfate species present in the probed solution (pointed out at 1105 cm⁻¹), and two kinds of sorbed sulfate distinguished by different Langmuir constants. The chemical nature of these two sorbed species is unclear, and the main reason of this interpretation is the good fit obtained on the adsorption isotherm. The spectral curve fitting of sulfate adsorbed onto hematite [12] was carried out by using three peaks (Fig. 3), according to an IS complex with a C_{3v} symmetry, two Lorentzians for the split ν_3 (1055 and 1130 cm⁻¹) and a Lorentzian for ν_1 (975 cm⁻¹). Spectra recorded on sulfate-treated goethite [11,60] were very similar to those obtained on hematite [12] but two Gaussian peaks attributed to an OS complex (degenerated ν_3 at 1108 cm⁻¹ and ν_1 at 975 cm⁻¹) were included along the Gaussian peaks coming from an IS complex with a C_{2v} (C₁) symmetry (ν_3 at 1170, 1133 and 1055 cm⁻¹, and ν_1 at 922 cm⁻¹) (Fig. 4).

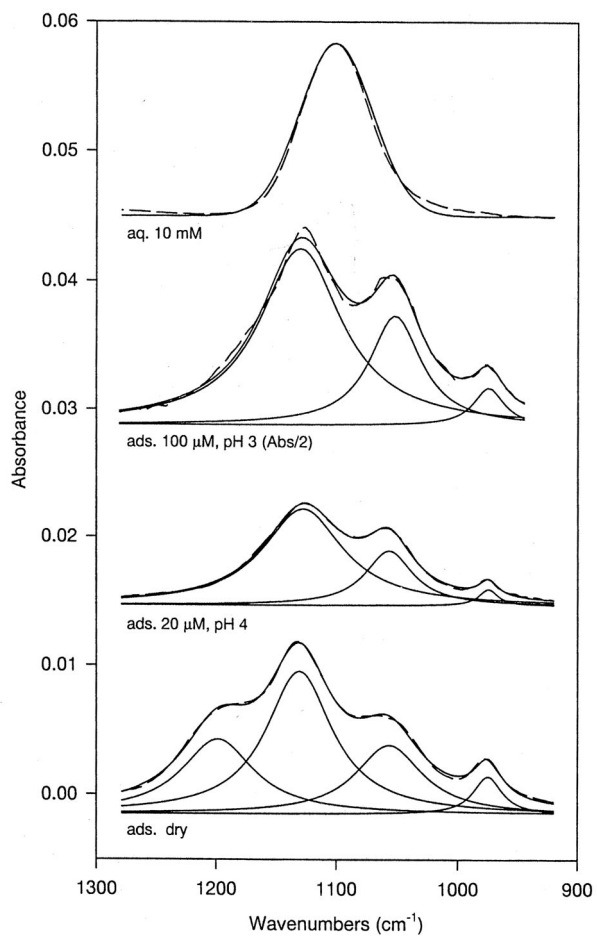


Fig. 3. ATR-FTIR spectra of sulfate adsorbed on hematite and curve fitting. The spectra are offset vertically for clarity. aq. refers to aqueous and ads. to adsorbed sulfate, followed by the aqueous concentrations. Dashed lines are the experimental spectra; solid lines are the fits (reprinted from *J. Colloid Interface Sci.* 188, S.H. Hug, In situ Fourier transform infrared measurements of sulfate adsorption on hematite in aqueous solutions, pp 415-422, copyright 1997, with permission from Elsevier [12]).

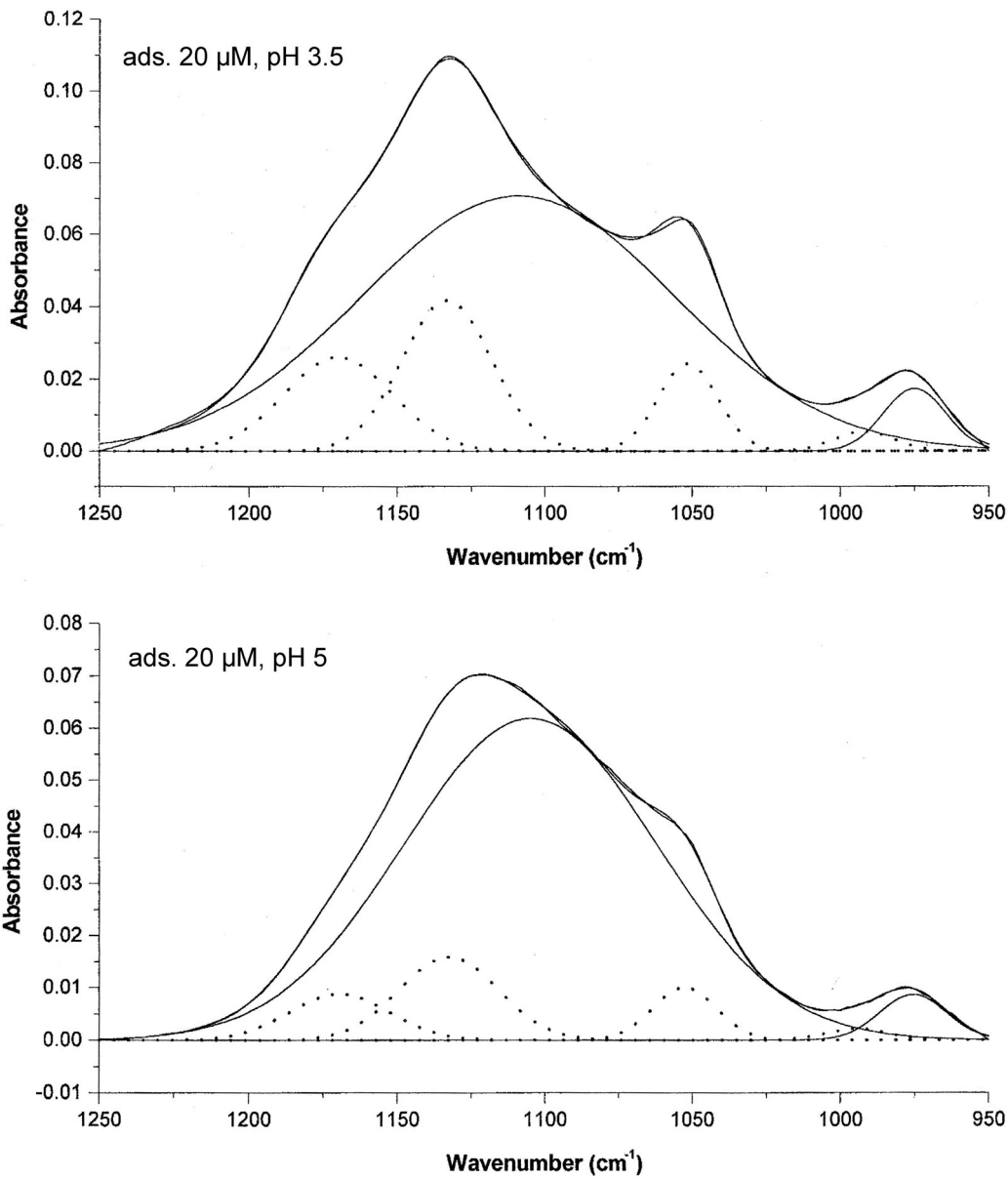


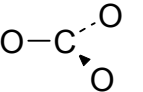
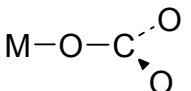
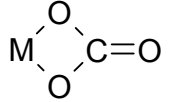
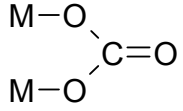
Fig. 4. ATR-FTIR spectra of sulfate adsorbed on goethite and spectral curve fitting. ads. refers to adsorbed sulfate, followed by the aqueous concentrations. The dotted lines denote the peaks arising from an inner-sphere complex (reprinted from J. Colloid Interface Sci. 218, D. Peak, R.G. Ford R.G. and D.L. Sparks, An in-situ FTIR-ATR investigation of sulfate bonding mechanisms on goethite, pp289-299, copyright 1999, with permission from Elsevier [11]).

Given the similarity between the spectra of sulfate adsorbed onto hematite and goethite, the difference of the conclusions obtained after the decomposition is striking.

Carbonate

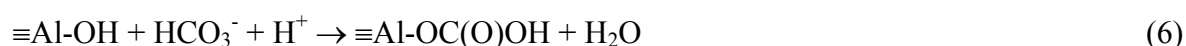
Sorption of carbonate ions on aluminum and iron oxides was found to be relatively weak, since it is strongly influenced by ionic strength and type of electrolyte anion [33,54]. However, its effect on the electrophoretic mobility is known [31] and resulting in the iep drop observed on oxides contaminated by carbonate impurity. The free CO_3^{2-} ion has a D_{3h} symmetry (trigonal planar) and its spectrum is dominated by the ν_3 band (asymmetric stretching) at 1385-1390 cm^{-1} [31,54]. Bicarbonate ion (HCO_3^-) has a C_{2v} symmetry leading to a strong band at 1360 cm^{-1} (symmetric stretching of CO_2 [31,54]) with a shoulder around 1300 cm^{-1} (COH bend [54]). At 1605 and 1668 cm^{-1} , two bands appear, assigned to the asymmetric stretching of CO_2 [31]. In aqueous solution, these latter bands can be obscured by the strong H_2O absorption. ATR-FTIR analyses were performed on samples of hydrous aluminum oxide (HAO) [31], hydrous ferric oxide (HFO) [31], goethite [31,33,34,61], hematite [36] and aged γ -alumina [54] after sorption of carbonate. The conclusion of these studies are identical for all studied substrates: carbonate ions form a monodentate complex at the surface [31,33,34,54,61]. The distinction between outer-sphere complex, monodentate, bidentate and bridging bidentate complexes is based on the degree of splitting of the $\nu_3(\text{CO})$ stretch vibration seen around 1500 cm^{-1} (named $\Delta\nu$ below). From the spectra of some Co(III)-carbonato complexes, the splitting criterion was described in table 5.

Table 5. $\Delta\nu_{\text{CO}}$ splitting for several coordination modes in Co(III) carbonato complexes
(adapted from ref. [54])

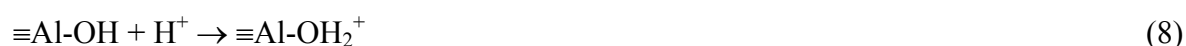
	Species geometry	Symmetry	$\Delta\nu$ (cm^{-1})
	aqueous carbonate	D_{3h}	0
	Monodentate	C_{2v}	80-110
	Bidentate binuclear	C_{2v}	310-340
	Bridging bidentate	C_{2v}	400-750

However, $\Delta\nu$ is correlated with the polarizing power of the cation (z/r^2 where z is the formal charge and r the ionic radius), what may prevent the comparison between $\Delta\nu$ measured for Co(III)-carbonato complexes and metal oxy-hydroxides surfaces if this parameter is very different. It is not the case for Al(III) and Fe(III) compounds, and the $\Delta\nu$ is expected to be comparable with the values obtained for the Co(III)-carbonato complexes. Results of determinations of $\Delta\nu$ are the following: 120 cm^{-1} for aged γ -alumina [54] (mainly bayerite β - $\text{Al}(\text{OH})_3$ in surface [62]), 70 cm^{-1} for HAO [31], 130 cm^{-1} for HFO [31], 75 [31], 155 [33], 164 cm^{-1} [34], or 195 cm^{-1} [61] for goethite, and 150 cm^{-1} for hematite [36]. All these values are clearly smaller than those measured for bidentate complexes (between 300 and 750 cm^{-1}) and may correspond to a monodentate complex. However, the ν_3 band gives no information on the protonation of the complex. Thus, carbonate can be sorbed as $\equiv\text{M}-\text{O}-\text{C}(\text{O})\text{O}^-$ or $\equiv\text{M}-\text{O}-\text{C}(\text{O})\text{OH}$. The main difference between the spectra of carbonate and bicarbonate ions is the presence of two bands around 1600 cm^{-1} for the latter species. Such bands in the spectrum of sorbed carbonate may reveal the protonation of the surface complex and this criterion was

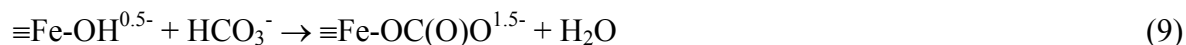
used in some studies [31,54] although the absorption of H₂O in this range complicates this method [33,54,61]. However, Wijnja and Schulthess have observed no significant bands around 1600 cm⁻¹ for sorbed carbonate onto a suspension of aged γ -alumina [54] or goethite [61] in D₂O and concluded that only a deprotonated surface complex of carbonate is present. A previous macroscopic study [63] has indicated that bicarbonate ions would be sorbed with a proton stoichiometry of 1:1, what would be consistent with the following reaction:



Since ATR spectra would indicate that the surface complex is deprotonated, the following concurrent adsorption reaction equation were proposed on aged γ -alumina surfaces [54]:



On goethite, the singly coordinated surface groups would concurrently react with bicarbonate ions and protons [61]:



Phosphate

Phosphate sorption was first studied by CIR-FTIR in goethite slurries [52], then by ATR in ferrihydrite suspensions [27] and on TiO₂ [26,32,48,64] or SiO₂ [26] thin layers. Spectra of phosphate solutions for different pH were recorded, and the stretching frequencies are listed in table 6.

Table 6. Positions of peak maxima of dissolved phosphate and symmetry of possible surface complexes

Species		Symmetry	IR active bands of solute species (cm ⁻¹)			
adsorbed*	solution					
outer sphere PO ₄ ³⁻	PO ₄ ³⁻	T _d	1006			
(MO)P(O)O	HPO ₄ ²⁻	C _{3v}	847-850	989	1077	
(MO) ₃ PO	H ₃ PO ₄		890	1006	1174-1179	
(MO) ₂ P(O)O	H ₂ PO ₄ ⁻	C _{2v}	870-874	940	1074-1075	1155-1160
(MO)P(O)(OH)O		C _s [32]				
(MO)P(O)(OH) ₂						
(MO) ₂ P(O)OH						
(MO) ₂ P(OH) ₂		C _{2v} or lower [27]				
(MO)P(O) ₂ OH						
[MOH ₂ ⁺]----						
	[(MO)PO ₃]					
[MOH ₂ ⁺]----						
	[(MO)P(O) ₂ OH]					
[MOH ₂ ⁺]----						
	[(MO)P(OH) ₂ O]					

* charge of the surface complexes are not indicated [27,32,52], --- stands for the bond

between hydrogen of hydroxyl and oxygen of phosphate complex [27]

PO₄³⁻ species show a single degenerated ν₃ asymmetrical vibration and there is no activation of the ν₁ (symmetric stretching) vibration [27]. For HPO₄²⁻ an H₃PO₄ species, ν₃ splits into two frequencies (respectively 1077, 989 and 1174-1179, 1006 cm⁻¹) and ν₁ band is activated (847-850 and 890 cm⁻¹). A reduction in the symmetry occurs for H₂PO₄⁻, leading to three bands for ν₃, along the activated ν₁ band. The possible surface inner-sphere complexes are numerous and their symmetry is mainly C_{2v} or lower, leading to four vibrational peaks.

Tejedor-Tejedor and Anderson [52], Arai and Sparks [27] and Gong [26] are tried to deduce the geometry of surface complexes from the spectra. On goethite [52] (Fig. 5), the spectra of phosphate sorbed is hindered by the stronger bands of lattice goethite groups at 894 and 800

cm^{-1} which prevents measurement at wavenumbers below 940 cm^{-1} .

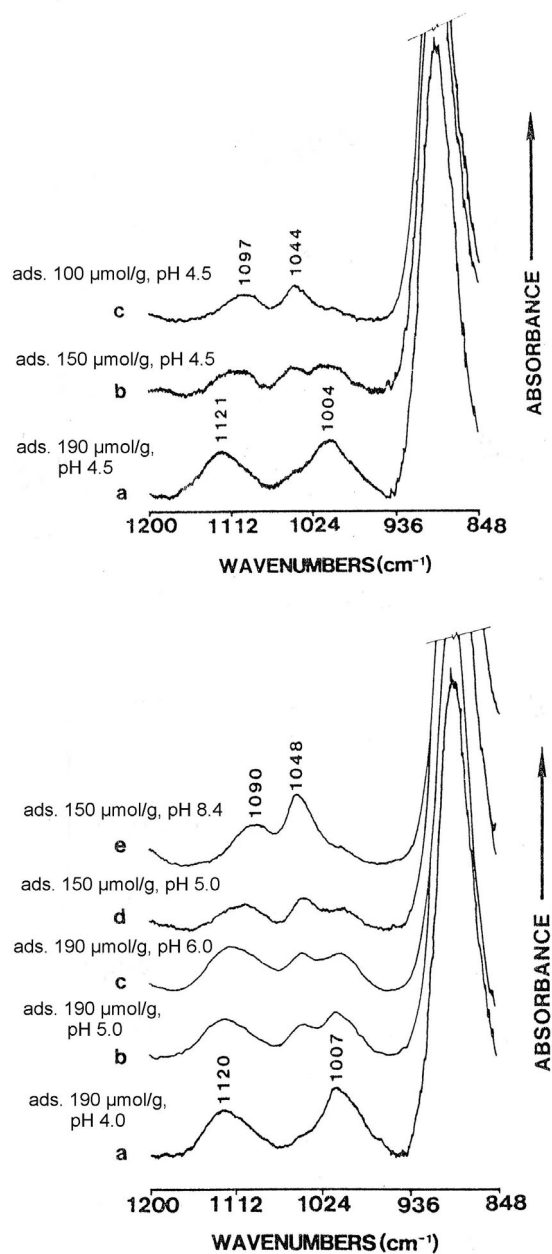


Fig. 5. Influence of phosphate surface coverage (top) and pH (bottom) on the CIR-FTIR spectra of phosphate sorbed on goethite (reprinted from Langmuir 6, M.A. Tejedor-Tejedor and M.I. Anderson, Protonation of phosphate on the surface of goethite as studied by CIR-FTIR and electrophoretic mobility, pp602-611, copyright 1990, with permission from American Chemical Society [52]).

The authors [52] have noted it is difficult to safely deduce the surface complex structure from the spectral results alone. They have shown the existence of three sets of bands: (I) 1123, 1006 and 982 cm^{-1} , (II) 1096 and 1044 cm^{-1} and (III) 1025 and 1001 cm^{-1} , they respectively attributed to $(\text{XO})_3\text{PO}$, $(\text{XO})_2\text{PO}_2$ and $(\text{XO})\text{PO}_3$ ($\text{X} = \text{H}$ or Fe) by comparison with spectra of aqueous phosphate whose frequencies decrease from $(\text{HO})_3\text{PO}$, $(\text{HO})_2\text{PO}_2^-$ to $(\text{HO})\text{PO}_3^{2-}$. A criterion based on the $\text{P}=\text{O}$ stretching was used to identify the first two surface complexes: the frequency of $\nu_{\text{P}=\text{O}}$ in $(\text{HO})_3\text{P}=\text{O}$ is 1174 cm^{-1} , and the higher band of (I) is low enough to correspond to a bidentate $(\text{FeO})_2(\text{HO})\text{PO}$ species. Thus (II) is attributed to $(\text{FeO})(\text{OH})\text{PO}_2$. On ferrihydrite, Arai and Sparks [27] decompose their spectra with three Gaussians (1088, 1021 and 952 cm^{-1}), whose distributions resemble those of H_2PO_4^- . Since no significant change in the position was seen in D_2O , a nonprotonated complex $(\text{FeO})_2\text{PO}_2$ is deduced. On TiO_2 , Gong [26] sorted the bands in the spectra into two groups: (I) 1115, 1055, 972 and 915 cm^{-1} and (II) 1008 cm^{-1} . The single band (II) resembles the spectrum of PO_4^{3-} and is attributed to an outer sphere complex. The former group is similar to the spectra of $(\text{HO})_2\text{PO}_2^-$ (1155, 1075, 940 and 874 cm^{-1}), and the difference is consistent with a bidentate surface complex whose $\nu_{\text{P}-\text{O}}$ (upper two frequencies) is lower since $\text{P}-\text{OTi}$ is stronger than $\text{P}-\text{OH}$, and $\nu_{\text{P}-\text{OH}}$ (lower two frequencies) is higher since $\text{TiOP}-\text{O}$ is weaker than $\text{HOP}-\text{O}$. On the same oxide, Connor and McQuillan [32] have fitted their spectra by two sets of four bands: (I) 1085, 1038, 970 and 890 cm^{-1} at high pH and (II) 1109, 1025, 936 and 890 cm^{-1} at low pH but this have not allowed them to conclusively identify the adsorbed species. As shown by this synthesis and as noticed by Connor and McQuillan [32], “the complexity of the band fitting for this system [oxide/phosphate] somewhat reduce the confidence in the conclusions reached from the derived data”. In order to obtain further information on the stability of monodentate and bidentate surface complexes, the adsorption of substituted phosphates was carried out [32]. n-butyl phosphate ($\text{BuP}(\text{O})\text{O}_2^{2-}$) was adsorbed whereas dimethyl phosphate ($\text{Me}_2\text{P}(\text{O})\text{O}^-$),

whose alkyl groups prevent it to form a bidentate complex with the surface, showed no adsorption onto TiO₂. The results of this experiment suggest that monodentate binding of phosphate species to TiO₂ surface is not viable. Such experiments with other substituted inorganic anions (methyl sulfate,...) could bring some direct information of the binding of the inorganic ions.

Indifferent ions

Numerous studies have dealt with the surface charge of inorganic colloids and particles, and with the methods used to obtain information. The surface charge created by the protonation/deprotonation of the hydroxyl groups for various pH is balanced by the ions present in the solution, creating a diffuse layer whose thickness is less than 3 nm for media whose ionic strength is higher than 0.01 M [1]. Thus, the evolution of the amount of these ions in function of the pH mirrors the surface charge of the solid. The use of IR active ions have allowed to McQuillan's group ([22] and references herein) to carry out surface titrations by internal reflection spectroscopy (STIRS). Solutions of tetramethylammonium perchlorate (TMA⁺ ClO₄⁻) 5 mM whose pH (2.3 – 11.7) was controlled by HClO₄ and TMA hydroxide were used to study TiO₂ [22] and chromium (III) oxy-hydroxide [24] films. Characteristic bands occurs at 1485 cm⁻¹ (antisymmetric CH₃ deformation of TMA⁺) and 1104 cm⁻¹ (antisymmetric $\nu_{\text{Cl-O}}$ of ClO₄⁻), and the evolution of their surface excess concentrations have led to an *iep* at pH 5 for TiO₂. For chromium oxy-hydroxide (expected *iep*: 7-8.5), no TMA⁺ concentration was observed, and ClO₄⁻ was only seen for pH lower than 5. The negative charge of the surface seems very small and another indifferent cation (Co(en)₃³⁺) with a higher charge was used and was detected (bands at 1585, 1470, 1164 and 1060 cm⁻¹) at the surface until pH 10.6. For the three ions (TMA⁺, ClO₄⁻ and Co(en)₃³⁺), it was checked that the

absorption bands of sorbed species are unchanged when compared with the spectra in aqueous solutions, indicating a simple electrostatic interaction with the surface. Wijnja and Schultess [54] have shown the spectra of nitrate sorbed at the alumina/water interface to illustrate this characteristics of a very weak interaction with the surface (bands at 1400 and 1348 cm^{-1}). By CIR-FTIR, Tejedor-Tejedor and Anderson [53] have recorded spectra of goethite in presence of ClO_4^- and NO_3^- to determine the influence of these ions in the structuration of water. Due to the method used to correct the background (subtraction of the supernatant spectra), the quality of the spectra is lower than those shown in previously described studies [22,24,54]. A doublet was seen for sorbed NO_3^- (1398 and 1346 cm^{-1}) and a band at 1095 cm^{-1} with a shoulder at 1164 cm^{-1} for ClO_4^- . The spectra of sorbed nitrate is the same as nitrate in solution [54] but the authors [53] expected only one band at 1390 cm^{-1} according to its D_{3h} symmetry, and explain the difference by the existence of $\text{Na}^+:\text{NO}_3^-$ ion pairs in solution.

Others inorganic ions (Se, As, B, $\text{S}_2\text{O}_3^{2-}$)

The adsorption of other inorganic ions on oxides was studied, but with few published works for each of them.

Thus, Degenhardt and McQuillan [24] showed spectra of $\text{S}_2\text{O}_3^{2-}$ adsorbed onto a chromium oxy-hydroxide layer. The free thiosulfate ion has a C_{3v} symmetry, and bands were observed at 1115 cm^{-1} (antisymmetric $\nu_{\text{S-O}}$) and 996 cm^{-1} (symmetric $\nu_{\text{S-O}}$). Thiosulfate adsorption was detected below pH 8 (a band at 1104 cm^{-1} with a shoulder at 1140 cm^{-1} , and a band at 994 cm^{-1}), leading to the conclusion that the adsorption is predominantly ionic [24].

Su and Suarez [29] have studied borate adsorption on amorphous aluminum and iron hydroxides. A lack of published IR data on boric acid solution have led the authors to analyze aqueous boric acid as a function of pH (7 - 11) and total B concentration. Tetrahedral $\text{B}(\text{OH})_4^-$

anion at pH 11 ($\text{pK}_a \text{B(OH)}_3/\text{B(OH)}_4^- = 9.14$ [21]) is characterized by a broad band at 1170 cm^{-1} (B-OH bending) and a band at 955 cm^{-1} (asymmetric stretching). For B(OH)_3 at pH 7, two bands at 1410 and 1148 cm^{-1} are seen, respectively assigned to B-O asymmetric stretching and B-OH in plane bending. The spectra of Al(OH)_3 paste at pH 7 with adsorbed B indicate trigonal boron environment with frequencies (1420 and 1280 cm^{-1}) higher if compared to the boric acid solutions. The strengthening of O-B and B-OH bonds in the surface complex $\equiv\text{Al-O-B(OH)}_2$ would explain this frequency evolution. At pH 10, two bands at 1412 and 1266 cm^{-1} were recorded, with a raising baseline from 1500 to 1200 cm^{-1} . In the range $1000\text{-}900 \text{ cm}^{-1}$, a strong band interference with Al-O bond from the solid occurs and prevents from recording the asymmetric stretching of B(OH)_4^- (955 cm^{-1}). However, the similarity between this spectrum with those of boron adsorbed at pH 7 indicates that the adsorption of the neutral B(OH)_3 species would be preferred, due to the charge repulsion (iep of $\text{Al(OH)}_3 = 9.3$ [29]) encountered by B(OH)_4^- ion. On amorphous Fe(OH)_3 complexes spectra were recorded after B adsorption, with bands at 1400 , 1293 , 1257 and 985 cm^{-1} at pH 7, and 1394 , 1334 , 1242 and 962 cm^{-1} at pH 10. Thus, both trigonal and tetragonal boron species would be present on the mineral surfaces, maybe resulting of a surface-promoted polymerization of boron species, since boric acid forms a series of polyanions in solution. The same authors [4] have studied by ATR the sorption of selenate (SeO_4^{2-}) and selenite (SeO_3^{2-}) on amorphous Fe(OH)_3 at pH 5. Selenate species in solution are characterized by a band at 872 cm^{-1} (asymmetric stretching of Se-O bond). Due to its T_d symmetry, its complexation by surface groups would lead to a decrease of its symmetry and to a splitting of the triply degenerated band (see detailed explanation for sulfate ions). A complex band (maximum at 879 cm^{-1} with shoulders at 890 and 824 cm^{-1}) was observed for selenate sorbed on Fe(OH)_3 , indicating an inner-sphere complex. The free SeO_3^{2-} ion has a C_{3v} symmetry, but its high pK_{a2} (7.31 [21]) leads to a mixture with HSeO_3^- in the pH range where its sorption on

$\text{Fe}(\text{OH})_3$ was observed ($\text{pH} < 10$). Thus, selenite aqueous solutions exhibit bands at 851, 822 and 731 cm^{-1} ($\text{pH} 8$), or 849 and 825 cm^{-1} ($\text{pH} 5$). The spectrum of selenite sorbed on $\text{Fe}(\text{OH})_3$ at $\text{pH} 5$ is characterized by two broad bands at 844 and 750 cm^{-1} , too weak to allow the identification of the sorbed species. Peak and Sparks [55] have recorded the spectra of selenate sorbed onto hematite in D_2O (Fig. 6) and the ν_3 splitting to two peaks at 880 and 850 cm^{-1} is described, with the ν_1 peak at 820 cm^{-1} becoming active. A monodentate selenate surface complex was assumed from this spectra [55].

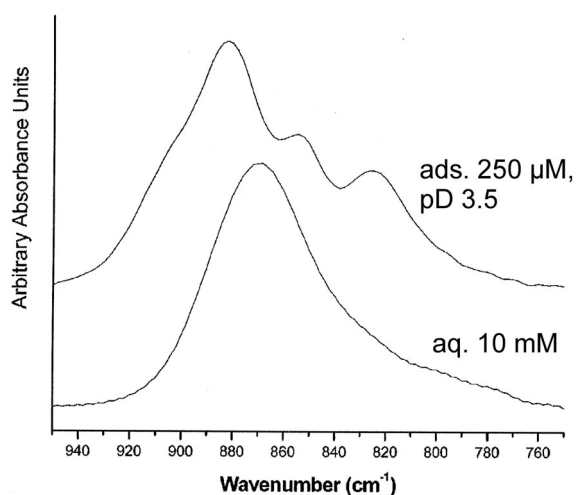


Fig. 6. ATR-FTIR spectra of selenate. ads refers to species adsorbed on hematite and aq. to aqueous SeO_4^{2-} (reprinted from Environ. Sci. Technol. 36, D. Peak, and D.L. Sparks, Mechanisms of selenate adsorption on iron oxides and hydroxides, pp 1460-1466, copyright. 2002, with permission from American Chemical Society [55]).

Arsenate ion (AsO_4^{3-}) sorption onto amorphous ferric oxide was studied by ATR [28]. The acidity constants of arsenic acid are 2.2, 6.9 and 11.5. Pure solution of arsenate ions are respectively characterized by bands at 792 cm^{-1} (AsO_4^{3-}), 858 cm^{-1} (HAsO_4^{2-}) and 908, 878 and 738 cm^{-1} (H_2AsO_4^-) [28]. Arsenate sorbed on a film of $\text{Fe}(\text{OH})_3$ at various pH have shown a band at $800\text{-}825 \text{ cm}^{-1}$ (shift toward lower frequency for higher pH values). From these

spectra and isotherm plots, a possible structure of bidentate, or weak bidentate via protonated oxide bridges was indicated [28].

Ternary complexes $\equiv\text{Fe}-\text{XO}_n^{m-}-\text{M}^{\text{X}}$

By combining results from ATR and EXAFS, information has been obtained on ternary systems goethite-sulfate-Pb(II) [30,60], goethite-carbonate-Pb(II) [34] and hematite-carbonate-U(VI) [36]. The main question is about the type of complex, characterized by the bridging ion, i.e. $\equiv\text{FeO}-\text{XO}_n^{m-}-\text{M}^{\text{X}}$ or $\equiv\text{FeO}-\text{M}^{\text{X}}-\text{XO}_n^{m-}$. For the goethite-sulfate-Pb(II) system, the addition of M^{X} ions in the suspension increases the signal of the oxoanion and modifies the spectra. Thus, the subtraction of the spectra recorded with and without metal leads to the spectrum of the sulfate bonded with the metal ion.

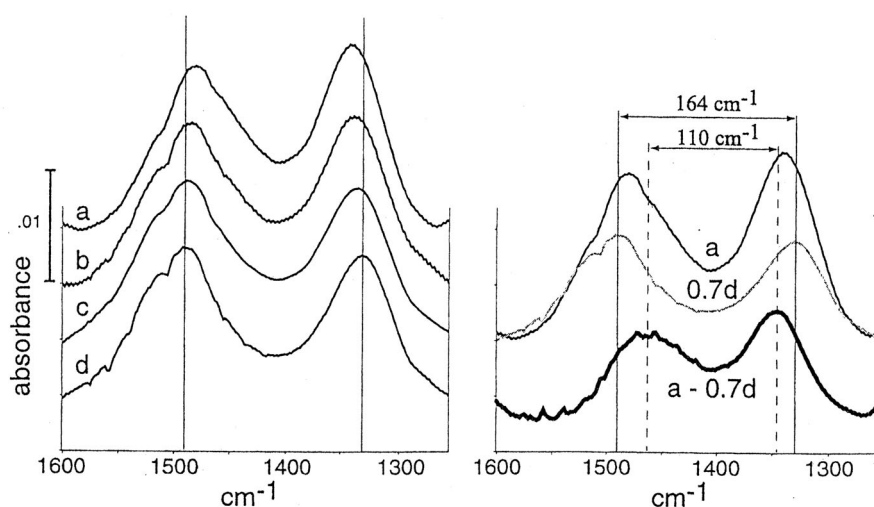


Fig. 7. ATR-FTIR spectra showing the effects of Pb on the ν_3 vibrations of carbonate sorbed to goethite. Pb surface coverages: 2, 1, 0.5 and 0 $\mu\text{mol}/\text{m}^2$ for spectra a-d respectively.

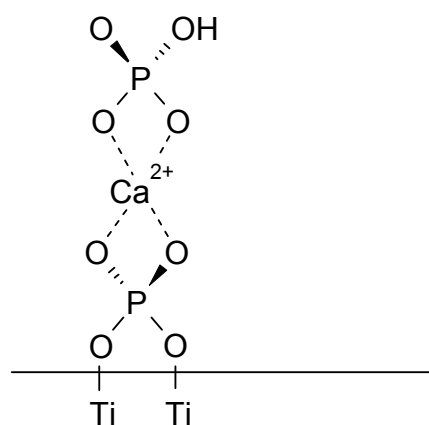
Spectrum at bottom right (bold) shows subtraction of Pb-free spectrum to highest coverage spectrum (reprinted from J. Colloid Interface Sci. 225, J.D. Ostergren, G.E. Brown, G.A.

Parks and P. Persson, Inorganic ligand effects on Pb(II) sorption to goethite ($\alpha\text{-FeOOH}$). II. Sulfate, pp483-493, copyright 2000, with permission from Elsevier [34]).

Ostergren et al. [60] identified the ternary complex as $(\equiv\text{Fe-O})_2\text{Pb-OSO}_3$, which is in agreement with the following similar study by Elzinga et al. [30].

A similar complex was found for the system goethite-carbonate-Pb(II), i.e. $(\equiv\text{Fe-O})_2\text{Pb-OCO}_2$ [34] (Fig. 7). For the system hematite-carbonate-U(VI), the data from ATR and EXAFS would be fitted by a $(\equiv\text{Fe-O})_2\text{UO}_2\text{-(CO}_3)_x$ complex, where $0 \leq x \leq 2$ [36].

Another case is the coadsorption of Ca^{2+} and phosphate on TiO_2 [64] where the presence of Ca^{2+} ions leads to an increased amount of adsorbed phosphate. This additional adsorbed phosphate would come from the formation of surface complex consisting in a bidentate phosphate bound to amorphous TiO_2 , with Ca^{2+} binding to the already adsorbed phosphate, and with an additional electrostatically adsorbed phosphate:



This conclusion is based on the difference between adsorption strength of Ca^{2+} and phosphate ions (adsorption of Ca^{2+} is weaker than phosphate), and on the decrease of the spectra structure in Ca^{2+} /phosphate sorption experiments, indicating a change of the adsorbed phosphate symmetry to C_{3v} (correlated to the electrostatically adsorbed HPO_4^{3-}). Experiments performed in the same conditions (CaCl_2 3.5×10^{-3} M, K_2HPO_4 3.8×10^{-3} M, pH 6.5) with crystalline TiO_2 (predominantly anatase), have shown that the precipitation of brushite ($\text{CaHPO}_4 \cdot 2 \text{H}_2\text{O}$) occurs. The difference between amorphous and crystalline TiO_2 towards Ca^{2+} /phosphate system is an important result for the knowledge of the growth of bone on titanium implants [64].

CONCLUSIONS AND FUTURE DIRECTIONS

The cited articles about the use of ATR-FTIR to study oxide/solution interface illustrate the possibility of this method to obtain in situ information on the sorbed species. It allows to bring elements to improve the comprehension of sorption mechanisms of some inorganic ions, differentiating between OS and IS complexes for example. Interpretation of the spectra to obtain information on IS complexation is more tricky due to the different possibilities of the spectra decomposition since reference spectra are difficult to obtain. This step is even more complex for ions able to sorbs with a lot of different geometries (phosphate for example). However, this method has several advantages suitable for the current problems in the sorption field: an in situ analysis, a sensitivity allowing the study of low surface coverage, and the possibility of time-resolved study. For five years, less than 20 articles have mentioned the use of ATR-FTIR to study the sorption of inorganic ions onto oxy-hydroxides amongst dozens of studies in this field. It illustrates the recentness of this technique and future developments should focus on some points that were less studied until now. Thus, ATR results have been hardly used to refine sorption modeling, even if it was an objective of the first studies [12]. The ionic strength is a usual parameter studied in batch experiments due to its effect on the OS sorption, but its influence on ATR spectra have been hardly investigated. When a mixture of OS and IS complexes is expected, it would be a way to help the decomposition of the spectra. Another point needing further investigation in studies using colloid layer onto ATR crystals is the effect of layer deposition protocol. The relation between amount of deposited colloid and signal intensity of sorbed species remains undocumented. The desorption of species from a colloid layer was rarely studied whereas a lack of reversibility was observed by Connor and McQuillan [32]. This behavior may result from the structure of the colloid film whose particles agglomerate to form micropores, what differs from well-stirred suspensions used in batch experiments. It would render difficult the comparison between sorption

experiments performed on a coated ATR element or on suspensions with a batch protocol. Thus, this point need to be clarified and new works about the characterization of the deposited layer would allow to define the limit of the use of the results from ATR.

ACKNOWLEDGEMENTS

The author thanks Sylvie Noinville (LADIR, Thiais, France) for assistance with ATR-FTIR technique, Catherine Droniou (CECM) for her help in getting bibliographic references, Michel Fédoroff (CECM) and A. James McQuillan (University of Otago, Dunedin, New Zealand) for discussion and helpful comments on a preliminary manuscript. Financial support from the Institut des Sciences Chimiques Seine-Amont (CNRS-IFR 1780) is gratefully acknowledged.

REFERENCES

- [1] W. Stumm, *Chemistry of the solid-water interface*, Wiley, New York, 1992.
- [2] J.F. Boily, in P. Somasundaran (Ed.), *Encyclopedia of Surface and Colloid Science*, Dekker, New York, 2002, p.3223.
- [3] J. Lützenkirchen, in P. Somasundaran (Ed.), *Encyclopedia of Surface and Colloid Science*, Dekker, New York, 2002, p.5028.
- [4] C. Su and D.L. Suarez, *Soil Sci. Soc. Am. J.* 64 (2000) 101.
- [5] K.F. Hayes, A.L. Roe, G.E. Brown, K.O. Hodgson, J.O. Leckie, and G.A. Parks, *Science* 238 (1987) 783.
- [6] D. Banerjee and H.W. Nesbitt., *Geochim. Cosmochim. Acta* 63 (1999) 1671.
- [7] R. Drot, E. Simoni, M. Alnot and J.J. Ehrhardt, *J. Coll. Interface Sci.* 205 (1998) 410.
- [8] J.R. Bargar, G.E. Brown, and G.A. Parks, *Geochim. et Cosmochim. Acta* 62 (1998) 193.
- [9] Y. Arai, E.J. Elzinga , and D.L. Sparks, *J. Colloid Interface Sci.* 235 (2001) 80.
- [10] C. Papelis, G.E. Brown, G.A. Parks and J.O. Leckie, *Langmuir* 11 (1995) 2041.
- [11] D. Peak, R.G. Ford and D.L. Sparks, *J. Colloid Interface Sci.* 218 (1999) 289.
- [12] S.H. Hug, *J. Colloid Interface Sci.* 188 (1997) 415.
- [13] T. Sugimoto, and Y. Wang, *J. Colloid Interface Sci.* 207 (1998) 137.
- [14] F.M. Mirabella, in F.M. Mirabella (Ed.), *Internal Reflexion Spectroscopy*, Dekker, New York, 1993, p.17.
- [15] J.W. Strojek, J. Mielczarski, and P. Nowak, *Adv. Colloid Interf. Sci.* 19 (1983) 309.
- [16] S.J. Hug, and B. Sulzberger, *Langmuir* 10 (1994) 3587.
- [17] A.R. Hind, S.K. Bhargava, and A. McKinnon, *Adv. Colloid Interf. Sci.* 93 (2001) 91.
- [18] J. Madejova, *Vib. Spectrosc.* 944 (2002) 1.

- [19] J.P. Coates, in F.M. Mirabella (Ed.), *Internal Reflexion Spectroscopy*, Dekker, New York, 1993, p.53.
- [20] L.D. Tickanen, M.I. Tejedor-Tejedor, and M.A. Anderson, *Langmuir* 7 (1991) 451.
- [21] *Handbook of Chemistry and Physics*, 79th ed.; D.R. Lide (Ed.), CRC Press, Boca Raton, 1998.
- [22] A.J. McQuillan, *Advanced Materials* 13 (2001) 1034.
- [23] J.D. Peak and D.L. Sparks, Kinetics of oxyanion sorption on metal oxides: a time-resolved ATR-FTIR spectroscopic study, *Proc. 5th Intern. Conf. on the Biogeochem. of Trace Metals*, Vienna, 1999, p344.
- [24] J. Degenhardt and A.J. McQuillan, *Langmuir* 15 (1999) 4595.
- [25] H. Wijnja and C.P. Schulthess, *J. Colloid Interface Sci.* 229 (2000) 286.
- [26] W. Gong, *Int. J. Miner. Process.* 63 (2001) 147.
- [27] Y. Arai, and D.L. Sparks, *J. Colloid Interface Sci.* 241 (2001) 317.
- [28] A.J. Roddick-Lanzilotta, A.J. McQuillan, A.J. and D. Craw, *Appl. Geochem.* 17 (2002) 445.
- [29] C. Su and D.L. Suarez, *Environ. Sci. Technol.* 29 (1995) 302.
- [30] E.J. Elzinga, D. Peak and D.L. Sparks, *Geochim. Cosmochim. Acta* 14 (2001) 2219.
- [31] C. Su and D.L. Suarez, *Clays Clay Miner.* 45 (1997) 814.
- [32] P.A. Connor and A.J. McQuillan, *Langmuir* 15 (1999) 2916.
- [33] M. Villalobos and J.O. Leckie, *J. Colloid Interface Sci.* 235 (2001) 15.
- [34] J.D. Ostergren, T.P. Trainor, J.R. Bargar, G.E. Brown and G.A. Parks, *J. Colloid Interface Sci.* 225 (2000) 466.
- [35] J.J. Lenhardt, J.R. Bargar and J.A. Davis, *J. Colloid Interface Sci.* 234 (2001) 448.
- [36] J.R. Bargar, R. Reitmeyer, and J.A. Davis, *Environ. Sci. Technol.* 33 (1999) 2481.
- [37] P.A. Connor, K.D. Dobson and A.J. McQuillan, *Langmuir* 11 (1995) 4193.

- [38] M. Janotta, M. Karlowatz, F. Vogt and B. Mizaikoff, *Anal. Chim. Acta* 496 (2003) 339
- [39] B.J. Ninness, D.W. Bousfield and C.P. Tripp, *Appl. Spectrosc.* 55 (201) 655
- [40] D.A. Dzombak and F.M.M. Morel, *Surface Complexation Modeling: Hydrous Ferric Oxide*, Wiley, New York, 1990.
- [41] W. Szczepaniak and H. Koscielna, *Anal. Chim. Acta* 470 (2002) 263.
- [42] G. Lefèvre, A. Walcarius, J.J. Ehrhardt, and J. Bessière, *Langmuir* 16 (2000), 4519.
- [43] R.P.J.J. Rietra, T. Hiemstra, and W.H. Van Riemsdijk, *J. Colloid Interf. Sci.* 229 (2000) 199.
- [44] A.E. Regazzoni, M.A. Blesa, and A.J.G. Maroto, *J. Colloid Interface Sci.* 122 (1988), 315.
- [45] R. Sprycha, *J. Colloid Interface Sci.* 102 (1984), 173.
- [46] J.M. Kleijn and J. Lyklema, *J. Colloid Interface Sci.* 120 (1987) 511.
- [47] R. Sprycha, *J. Colloid Interface Sci.* 127 (1989) 1.
- [48] A. Michelmore, W. Gong, P. Jenkins and J. Ralston, *J. Phys. Chem. Chem. Phys.* 2 (2000) 2985.
- [49] L. Celi, E. Barberis, and M. Franco Ajmone, *Soil. Sci.* 165 (2000) 657.
- [50] N.F. Gray, *Wat. Res.* 32 (1998) 2122.
- [51] Council Directive 98/83/EC on the quality of water intended for human consumption, European Union, 1998.
- [52] M.I. Tejedor-Tejedor and M.A. Anderson, *Langmuir* 6 (1990) 602.
- [53] M.I. Tejedor-Tejedor and M.A. Anderson, *Langmuir* 2 (1986) 203.
- [54] H. Wijnja, and C.P. Schulthess, *Spectrochimica Acta A* 55 (1999) 861.
- [55] D. Peak and D.L. Sparks, *Environ. Sci. Technol.* 36 (2002) 1460.
- [56] P. Persson and L. Lövgren, *Geochim. Cosmochim. Acta* 60 (1996) 2789.

- [57] K. Nakamoto, *Infrared and Raman spectra of inorganic and coordination compounds*, 4th ed., Wiley & Sons, New York, 1986.
- [58] C.G. Barraclough and M.L. Tobe, *J. Chem. Soc.* (1961) 1961.
- [59] R.L. Parfitt, and R.S.C. Smart, *Soil Sci. Soc. Am. J.* 42 (1978) 48.
- [60] J.D. Ostergren, G.E. Brown, G.A. Parks and P. Persson, *J. Colloid Interface Sci.* 225 (2000) 483.
- [61] H. Wijnja, and C.P. Schulthess, *Soil Sci. Soc. Am. J.* 65 (2001) 324.
- [62] G. Lefèvre, M. Duc, P. Lepeut, R. Caplain, and M. Fédoroff, *Langmuir* 18 (2002) 7530.
- [63] C.P. Schulthess, K. Swanson, and H. Wijnja, *Soil Sci. Soc. Am. J.* 62 (1998) 136.
- [64] T.K. Ronson and A.J. McQuillan, *Langmuir* 18 (2002) 5019.